Multistep Virtual Screening for Rapid and Efficient Identification of Non-Nucleoside Bacterial Thymidine Kinase Inhibitors

Johannes Zander,[b] Markus Hartenfeller,[a] Volker Hähnke,[a] Ewgenij Proschak,[c] Silke Besier,[b] Thomas A. Wichelhaus,[b] and Gisbert Schneider*[a]

Abstract: Antimicrobial activity of trimethoprim/sulfamethoxazole (SXT) against *Staphylococcus aureus* (*S. aureus*) is antagonized by thymidine, which is abundant in infected or inflamed human tissue. To restore the antimicrobial activity of SXT in the presence of thymidine, we screened for small-molecule inhibitors of *S. aureus* thymidine kinase with non-nucleoside scaffolds. We present the successful application of an adaptive virtual screening protocol for novel antibiotics using a combination of ligand- and structure-based approaches. Two consecutive rounds of virtual screening and in vitro testing were performed that resulted in several non-nucleoside hits. The most potent compound exhibits substantial antimicrobial activity against both methicillin-resistant *S. aureus* strain ATCC 700699 and nonresistant strain ATCC 29213, when combined with SXT in the presence of thymidine. This study demonstrates how virtual screening can be used to guide hit finding in antibacterial screening campaigns with minimal experimental effort.

Keywords: antibiotics · drug design · drug resistance · molecular modeling · protein models

Introduction

Staphylococcus aureus (*S. aureus*) causes multiple diseases ranging in severity from minor skin infections to life-threatening conditions, such as endocarditis, pneumonia, and sepsis.[1] Methicillin-resistant *S. aureus* (MRSA) has been widespread and has become a serious pathogenic bacterium, leading to high morbidity and mortality.[2,3] MRSA is not only resistant to treatment with ß-lactams, but often also to other antibiotics such as aminoglycosides, macrolides, lincosamides, and fluoroquinolones, because many MRSA strains possess a multidrug resistant genotype. Moreover, the appearance of vancomycin and linezolid resistance limited options for therapy against MRSA.[4,5] This evolution points to an urgent need for new anti-MRSA compounds and for the optimization of established ones with high antimicrobial activity.

Folic acid antagonists, such as trimethoprim/sulfamethoxazole (SXT), possess a wide antimicrobial spectrum and show good antimicrobial activity against *S. aureus* including MRSA.[6,7] These bioactive agents inhibit different enzymatic steps of the folic acid pathway leading to cessation of the bacterial synthesis of deoxythymidine monophosphate (dTMP) by thymidylate synthase. However, several bacterial species including *S. aureus* possess an alternative pathway for synthesis of intracellular dTMP by uptake of extracellular thymidine and subsequent intracellular phosphorylation to dTMP. Thus, the effect of folic acid antagonists can be antagonized by a high extracellular thymidine concentration as detected in tissues with necrotic cells such as pus and sputum from cystic fibrosis patients.[8–10] Indeed, there are several reports of unsuccessful treatment with folic acid antagonists, supposedly due to elevated thymidine concentrations in human tissues containing necrotic cells.[9,11,12]

We recently showed that, in the presence of thymidine, simultaneous inhibition of the folic acid pathway by SXT and the bacterial thymidine kinase (TK; EC 2.7.1.21) by nucleoside analogues, especially halogenated 2′-deoxyuridine derivatives, results in synergistic antimicrobial activity against

[a] M. Hartenfeller,+ V. Hähnke, Prof. Dr. G. Schneider
Eidgenössische Technische Hochschule (ETH)
Institute of Pharmaceutical Sciences
Wolfgang-Pauli Strasse 10, 8093 Zurich (Switzerland)
Fax: (+41) 44-633-1379
E-mail: gisbert.schneider@pharma.ethz.ch

[b] Dr. J. Zander,+ Dr. S. Besier, Prof. Dr. T. A. Wichelhaus
Institute of Medical Microbiology and Infection Control
Hospital of Goethe-University
Paul-Ehrlich-Strasse 40, 60596 Frankfurt/Main (Germany)

[c] Dr. E. Proschak
Institute of Pharmaceutical Chemistry
LIFF/OSF, Max-von-Laue-Strasse 9
Goethe-University Frankfurt, 60348 Frankfurt (Germany)

[+] Both authors contributed equally to this work.

S. aureus.[10] Halogenated 2′-deoxyuridine derivatives such as 5-chloro-2′-deoxyuridine (5-CldU) and 5-iodo-2′-deoxyuridine (5-IdU) have been shown to inhibit bacterial TK.[13,14] However, nucleoside analogues can be associated with cytotoxicity when phosphorylated to triphosphates and incorporated into DNA, thereby leading to single-strand breaks.[15,16] Screening for non-nucleoside analogues as potential thymidine kinase inhibitors is therefore of particular interest for the development of novel antibiotics.

This study was aimed at 1) screening for non-nucleoside analogue inhibitors of *S. aureus* thymidine kinase by multistep virtual screening, and 2) determining the in vitro activity of these thymidine kinase inhibitors against *S. aureus* in combination with SXT in the presence of thymidine.

ture of *Sa*TK in the presence of a natural ligand (thymidine) is not known, we used the structure of *Bacillus anthracis* thymidine kinase (*Ba*TK, PDB identifier: 2j9r, resolution: 2.7 Å)[20] as template for this purpose as the best available model. A sequence alignment between *Ba*TK and *Sa*TK exhibits sequence identity of 63 % overall and 100 % in the thymidine binding-site residues (Figure 1). Consequently,

```
S. aureus (ATCC 700699/ATCCC 29213)                MYETYHSGWIECITGSMFSGKSEELIRRLRRGIYAKQ
B. anthracis (PDB: 2j9r)                    SH__MYLINQNGWIEVICGSMFSGKSEELIRRVRRTQFAKQ
B. anthracis (complete)     MGSSHHHHHHSSGLVPRGSHMYLINQNGWIEVICGSMFSGKSEELIRRVRRTQFAKQ

S. aureus (ATCC 700699/ATCCC 29213)  KVVVFKPAIDDRYHKEKVVSHNGNAIEAINISKASEIMTHNLTNVDVIGIDEVQFFD
B. anthracis (PDB: 2j9r)             HAIVFKPCVK_____AVPVSASKDIFKHITEEMDVIAIDEVQFFD
B. anthracis (complete)              HAIVFKPCIDNRYSEEDVVSHNGLKVKAVPVSASKDIFKHITEEMDVIAIDEVQFFD

S. aureus (ATCC 700699/ATCC 29213)   DEIVSIVEKLSADGHRVIVAGLDMDFRGEPFEPMPKLMAVSEQVTKLQAVCAVCGSS
B. anthracis (PDB: 2j9r)             GDIVEVVQVLANRGYRVIVAGLDQDFRGLPFGQVPQLMAIAEHVTKLQAVCSACGSP
B. anthracis (complete)              GDIVEVVQVLANRGYRVIVAGLDQDFRGLPFGQVPQLMAIAEHVTKLQAVCSACGSP

S. aureus (ATCC 700699/ATCC 29213)   SSRTQRLINGKPAKIDDPIILVGANESYEPRCRAHHIVAPS
B. anthracis (PDB: 2j9r)             ASRTQRLIDGEPAAFDDPIILVGASESYEPRCRHCHAVPTKQ
B. anthracis (complete)              ASRTQRLIDGEPAAFDDPIILVGASESYEPRCRHCHAVPTKQR
```

Figure 1. Sequence alignment of thymidine kinases. The first two sequences represent the alignment that was used for the homology model (63 % sequence identity). PDB entry 2j9r of *B. anthracis* thymidine kinase misses some parts of the complete sequence (highlighted by black boxes and white letters) in the complete protein sequence, third line. A continuous gap was inserted at the corresponding position. Complete sequence identity of binding pocket residues (gray boxes) can be observed.

Results and Discussion

Substances that interact with viral and human thymidine kinases have been studied for many decades and several compounds have been found that exhibit high antiviral or anticancer activity.[17,18] In contrast, inhibitors of bacterial thymidine kinases have not attracted much attention in antibacterial research.[10,15,19,20] In most bacteria intracellular dTMP can be synthesized by two different pathways, which suggests combinations of bioactive agents inhibiting both pathways simultaneously.[10] Thymidine kinase inhibitors impair the salvage pathway for dTMP, which is initiated by thymidine kinase catalyzing the transfer of a gamma-phosphate group from adenosine-5′-triphosphate (ATP) to thymidine.[21] Folic acid antagonists inhibit different enzymatic steps of the bacterial synthesis of methylenetetrahydrofolate, an essential cofactor of thymidylate synthase for generation of dTMP from deoxyuridine monophosphate (dUMP). Simultaneous inhibition of both pathways therefore results in an intracellular lack of dTMP[22] and synergistic antimicrobial activity in the presence of thymidine.[10]

Comparative protein model: Here we used a virtual screening protocol to find potential thymidine kinase inhibitors with non-nucleoside structures. A crucial step of our screening protocol comprised automated docking of selected compounds into a homology model of *S. aureus* thymidine kinase (*Sa*TK). Several bacterial thymidine kinases can be crystallized, such as thymidine kinases from *S. aureus* (*Sa*TK, PDB identifier: 3e2i), *Ureaplasma urealyticum*, *Bacillus cereus*, and *Bacillus anthracis*.[13,20,23] As a crystal struc-

the resulting homology model (*Sa*TK) shows excellent structural agreement with the template (*Ba*TK), especially in the thymidine binding site (Figure 2). A continuous sequence stretch from *Ba*TK comprising 17 residues is missing in the template structure. This part is predicted to form a helix in the homology model of *Sa*TK. TKs of ATCC 29213 and ATCC 700699 have perfect sequence identity. This justifies employing one homology model for both proteins.

We explicitly did not perform docking studies on an existing crystal structure of *Sa*TK (PDB identifier: 3e2i).[23] The need for a homology model regardless of an existing structure of the target protein is rationalized by the fact that the structure of *Sa*TK has been crystallized in its *apo* form (i.e., no bound thymidine). It was shown that TKs of several microorganisms undergo substantial structural changes in a loop region forming the upper part of the binding pocket upon thymidine binding.[24] This renders the existing X-ray structure of the *Sa*TK in its *apo* form unsuitable for docking efforts. It is therefore not surprising that a comparison between the homology model of *Sa*TK and the respective crystal structure of the *apo* form exhibits a relatively high root-mean-square deviation (RMSD) of 3.9 Å. This finding originates from 1) a deviation in the position of the loop region of *Sa*TK that depends on the missing ligand binding and 2) the fact that a part of the sequence corresponding to the one missing in the template structure of *Ba*TK is also absent in the structure of the *Sa*TK *apo* form (Figure 3).
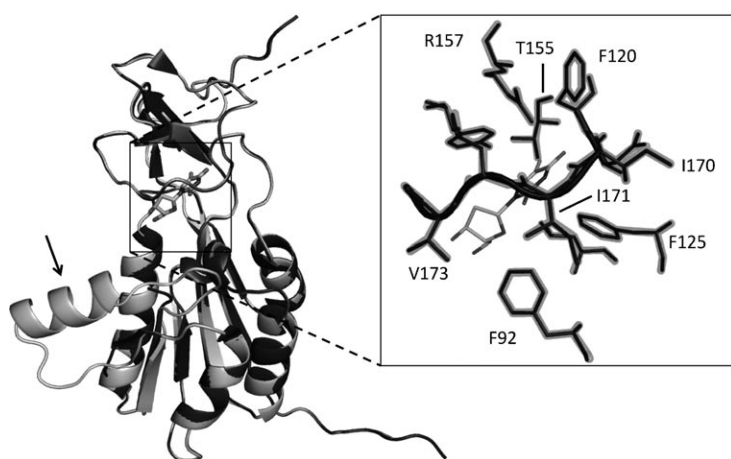
Figure 2. Binding-site model of *Sa*TK. Left: Comparison of a homology model of *S. aureus* thymidine kinase and the template structure of *B. anthracis* thymidine kinase (PDB entry: 2j9r, chain A), together with bound native ligand thymidine. The missing part of the template (cf. Figure 1) is predicted to form a helix (arrow) flanked by two loop regions. Right: Perfect alignment between amino acid side chains of the model (transparent) and the template (solid). Identifiers of selected pocket residues of the model and a short stretch of the backbone (sketched) are shown for orientation.
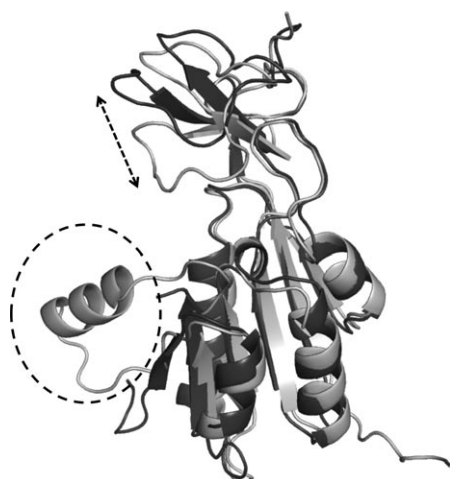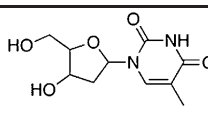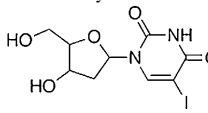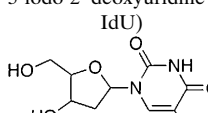

Figure 3. Comparative "homology" model of *Sa*TK. Comparison of the homology model of *S. aureus* thymidine kinase (light gray) and an existing X-ray *apo* structure of the same protein (dark gray, PDB entry: 3e2i). Structural difference can be found mainly in the position of the loop defining the upper part of the binding cavity upon ligand binding (arrow). Bound glycerol (not shown) does not populate the thymidine binding pocket in structure 3e2i. As within the structure of thymidine kinase of *B. anthracis* that was used as template for homology modeling, an equivalent part of structure 3e2i is missing (dashed circle).

Reference ligands: For our ligand-based screening efforts we used 5-chloro-2′-deoxyuridine (5-CldU, **3**) with a minimal inhibitory concentration (MIC) of 0.0625 mg L^{-1} against both *S. aureus* strains when combined with SXT in the presence of thymidine (**1**). The same MICs were determined for 5-iodo-2′-deoxyuridine (5-IdU, **2**), another ligand of bacteri-

al thymidine kinase.[14] SXT alone in the presence of thymidine showed MIC values of >128 mg L^{-1} against both *S. aureus* strains (not shown). 5-CldU and 5-IdU were chosen as reference ligands because halogenated 2′-deoxyuridine derivatives have recently been reported as thymidine kinase inhibitors showing significantly improved antimicrobial activity against *S. aureus* when combined with SXT in the presence of elevated thymidine concentrations.[10] Moreover, Kosinska and co-workers showed that thymidine kinase from *Ureaplasma urealyticum* exhibits pronounced phosphorylation activity with 5-CldU as substrate.[13] In a first study, we re-docked the natural ligand thymidine and the screening reference 5-CldU to obtain a reference value for the assessment of docking scores and to evaluate the performance of our docking protocol. Notably, automated ligand docking was able to reproduce the binding pose of thymidine. Thymidine and 5-CldU achieved favorable comparable docking scores of 37 and 38, respectively (higher docking scores suggest better ligand binding; Table 1).

Table 1. Reference compounds and values. Minimal inhibitory concentration (MIC) values measured for both *S. aureus* strains, and docking scores.

Structure	MIC [mg L^{-1}]		Docking score (ASP)
	ATCC 700699	ATCC 29213	
1 thymidine	–	–	37
2 5-iodo-2′-deoxyuridine (5-IdU)	0.0625	0.0625	38
3 5-chloro-2′-deoxyuridine (5-CldU)	0.0625	0.0625	38

Virtual screening protocol: We followed a stepwise virtual screening protocol (Figure 4). A diverse screening library containing approximately 557 000 readily available compounds from two different suppliers was prepared. The first virtual screening step consisted of a rigorous reduction of the screening library ("negative design") by similarity analysis of pool compounds with the reference ligand 5-CldU (Table 1). For this purpose an in-house implementation of a self-organizing map (SOM)[25] was employed to map the screening pool (represented in a high-dimensional space spanned by uncorrelated molecular descriptors) to a two-dimensional (2D) regular grid, as described.[26] The SOM allowed for the identification of a cluster of 912 compounds
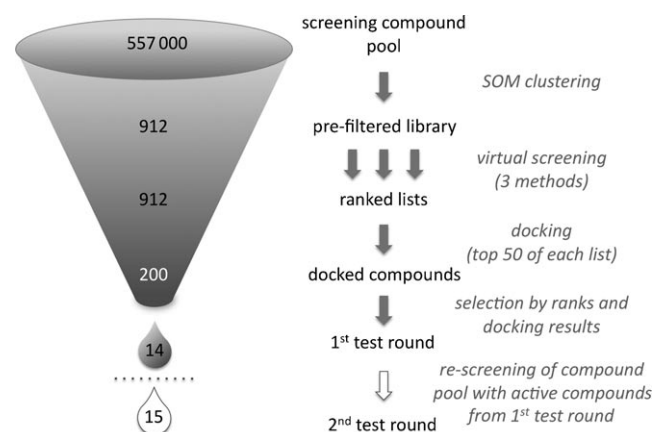
Figure 4. Virtual screening protocol. The second test round was performed on the complete screening compound library with the best hits from the first screening round.

that exhibit high similarity to the reference compound ("positive design").

These candidate ligands were considered for the next screening steps. Three ligand-based screening techniques—each one focusing on a different aspect of ligand similarity—were applied on this small pre-filtered compound collection with respect to the same reference ligand (5-CldU):

1) The pharmacophore alignment search tool (PhAST)[27] compares molecules by aligning strings of pharmacophoric feature types devised from their 2D representation.
2) Pseudoreceptor point similarity (PRPS)[28] computes pseudoreceptor representations of molecules based on three-dimensional (3D) conformations.
3) ShaEP[29] calculates a similarity score by comparing 3D conformers with respect to spatial overlap of shape and electrostatic potentials.

PhAST was applied in two different modes of structure canonization (for more information, see the Experimental Section) resulting in a total of four individual screening runs. Each method provided us with a sorted list of the remaining 912 screening compounds, ranked according to the scoring

schemes of the methods. Molecules ranked among the top 50 of each individual list were subsequently docked into a homology model of *S. aureus* thymidine kinase. Compounds from the top scoring ranks with plausible docking poses yielding high docking scores and hydrogen bridges similar to the reference ligands were considered for further investigation. We selected and ordered 14 compounds, which were tested in vitro for their biological activity on *S. aureus* thymidine kinase. A bacterial whole-cell assay was chosen to see whether virtual screening can cope with antibacterial activity without explicitly predicting this property. Out of the 14 tested compounds, seven compounds (**4–10**) exhibit antimicrobial activity against *S. aureus* strain ATCC 700699 and *S. aureus* ATCC 29213 when combined with SXT in the presence of thymidine (Table 2). None of these compounds had any intrinsic antimicrobial activity (data not shown). The fact that 50% of the 14 compounds chosen for in vitro screening showed antimicrobial activity when combined with folic acid antagonists argues for an effective first screening round. Based on the findings of the first screening two parallel strategies were applied to select compounds in a second screening round:

1) A second pseudoreceptor model using our software PRPS was employed to screen the complete compound

Table 2. Results of the first round of virtual screening and in vitro tests. MIC values represent the median of three experiments.

Structure	MIC [mg L^{-1}]		Docking score (ASP)	Virtual screening rank			
	ATCC 700699	ATCC 29213		P1[a]	P2[b]	PRPS	ShaEP
4	128	128	36	3	2	–	–
5	128	128	38	11	41	–	–
6	128	128	39	17	18	–	–
7	128	>128	31	–	–	2	–
8	128	128	26	–	–	6	–
9	32	64	42	–	8	5	–
10	32	64	41	–	–	–	18

[a] PhAST with Isomap canonization. [b] PhAST with Prabhakar canonization (cf. Experimental Section).

library ($\approx 557\,000$ molecules) again. The model was built from all seven active compounds found in the first screening round. Reference compounds were aligned according to their docking poses.
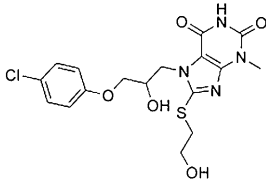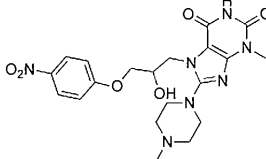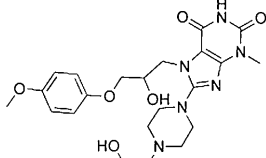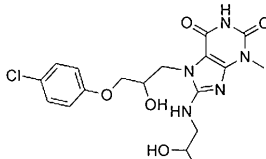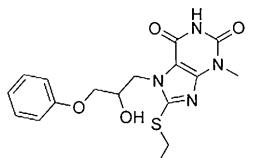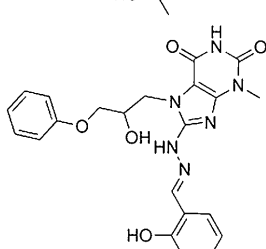
2) Compound **10** contains a catechol moiety that is buried deep inside the thymidine binding site according to the docking hypothesis. This "head group" is of particular interest as it is structurally distinct from nucleosides. Therefore, we performed a substructure search for compounds featuring this head group.

The top-scoring 100 molecules of the PRPS screening with the second pseudoreceptor model were docked into the homology model, and seven compounds were selected for testing, from which six compounds (**11–16**) exhibit antimicrobial activity in combination with SXT. Compound **16** has higher activity than the best compounds **9** and **10** found in the first screening round (Table 3). In addition, we retrieved 50 compounds containing the head group identified as promising in round one and docked them into the homology model. Compounds **17–24** were selected for testing according to plausibility of generated poses, high docking scores, and structural variations of the "tail group". All eight substances exhibit the desired effect (hit rate 100%) with six compounds showing improved MIC values with respect to compounds of test round one. The most potent compound, **24**, exhibits a MIC value of $0.25\,\mathrm{mg\,L^{-1}}$ on both *S. aureus* strains when combined with SXT in the presence of thymidine, which is only fourfold less potent than 5-CldU and 5-IdU (Table 4). Again, docking of **24** suggests that the head group is buried in the binding pocket while the methylquinoline tail group interacts with the protein surface outside the cavity (not shown).

Compound **24** has a rather poor ligand efficiency[30] [$LE = -\ln(MIC)/(\text{no. of non-hydrogen atoms})$] of 0.06. For both reference compounds, 5-IdU and 5-CldU, we obtained an LE value of 0.16. Although the primary aim of this work was to identify non-nucleoside inhibitors of *Sa*TK, the motivating findings suggest that there is room for further optimization with respect to both binding affinity and molecular mass.

Five compounds (**19**, **20**, **21**, **23**, **24**) exhibit intrinsic antimicrobial activity. MICs of these compounds in the presence of thymidine against *S. aureus* strains ATCC 29213 and ATCC 700699 are given in Table 5. MICs are substantially higher than those obtained in combination with SXT. The fact that the substances tested in this study showed no or only weak intrinsic antimicrobial activity is consistent with mainly thymidine kinase inhibition. It is known that some thymidine kinase inhibitors such as 5-fluoro-2′-deoxyuridine also inhibit thymidylate synthase and as a consequence have intrinsic antimicrobial activity.[15] Future studies aiming at hit-to-lead structure optimization should use direct bacterial thymidine kinase inhibition assays to verify thymidine kinase being the target of these non-nucleoside antibiotics.

Table 3. Screening results of the second PRPS model based on the active compounds of the first round. MIC values represent the median of three experiments.

Structure	MIC [mg L⁻¹]		Docking score (ASP)
	ATCC 700699	ATCC 29213	
11	128	128	45
12	128	128	41
13	128	128	41
14	64	128	42
15	32	128	43
16	16	16	45

Conclusion

Our study demonstrates that multistep virtual screening can help identify bioactive substances from a large screening compound pool with limited experimental effort. Rapid focusing on promising candidate structures was possible, so that inhibitors of bacterial thymidine kinase with non-nucleoside scaffolds were identified. These inhibitory compounds exhibit moderate to high antimicrobial activity when combined with folic acid antagonists in the presence of thymidine, and provide rich opportunity for further optimization. Notably, at least two subsequent screening rounds were

Table 4. Results of substructure screening. The dihydroxyphenyl head group is preserved in all active molecules. MIC values represent the median of three experiments.

	Structure	MIC [mg L^{-1}]		Docking score (ASP)
		ATCC 700699	ATCC 29213	
17		128	>128	37
18		128	128	39
19		16	8	43
20		8	8	46
21		4	2	41
22		4	2	45
23		1	1	38
24		0.25	0.25	39

Table 5. Intrinsic antimicrobial effect of non-nucleoside analogues. MIC values were measured in the presence of thymidine (200 μg L^{-1}) and absence of SXT against both *S. aureus* strains. Values are medians of three experiments.

	MIC [mg L^{-1}]	
	ATCC 700699	ATCC 29213
19	128	128
20	64	128
21	64	64
23	16	32
24	32	32

required to yield potent hits. The trick was to use information gained about the structuring of the chemical space spanned by the screening compound pool for "adaptive" optimization based on iterative learning.[31] We suggest explo-

ration of the full potential of adaptive multistep and multimethod virtual screening in early drug discovery projects,[32] which might speed up the transition from biological target validation to chemical hit and lead structure optimization.

Experimental Section

Strains and genetic sequence determination of bacterial thymidine kinase: *S. aureus* strain ATCC 700699 is resistant to methicillin (MRSA) and exhibits reduced susceptibility to vancomycin.[33] The genetic sequence of its thymidine kinase-encoding tdk gene was published in 2001 as part of the whole genome sequence.[34] Methicillin-susceptible *S. aureus* strain ATCC 29213 serves as a quality-control strain for antibiotic susceptibility testing.[35] The chromosomal tdk gene of *S. aureus* strain ATCC 29213 was amplified by polymerase chain reaction (PCR) with forward primer P1 (5′-GCGAT-TATGTTTTGAAAAAGGTGG-3′) and reverse primer P2 (5′-GTTCGTATCTTTCTTCTACAA-TATC-3′). The nucleotide sequence of the tdk gene of *S. aureus* ATCC 29213 was determined by cycle sequencing using an ABI PRISM DNA sequencer (Applied Biosystems, Foster City, USA).

Compound library: Virtual screening was performed with a structurally diverse set of compounds from supplier catalogues of Specs (v01/2009, Specs, Delft, The Netherlands) and Asinex Gold and Platinum collections (v11/2008, Asinex, Moscow, Russia). Protonation states of all compounds were standardized ("washed") using the "wash" function of MOE (v2008.10, Chemical Computing Group, Montreal, QC, Canada). Single three-dimensional conformations for each screening compound were computed with the software CORINA (v3.2, Molecular Networks, Erlangen, Germany).

Self-organizing map: The reference compound 5-CldU was added to the screening library before the calculation of all 184 2D descriptors of MOE for each molecule. Principal component analysis[36] revealed that 95% of the variance in the dataset could be explained using the 40 first principal components, so these uncorrelated descriptors were used for representing the screening compound library. We used an implementation of the self-organizing map (SOM)[25] algorithm to further reduce the dimensionality of the dataset.[26] The SOM performed a nonlinear mapping from the original descriptor space (here: 40-dimensional) on a two-dimensional map. Each molecule is assigned to one of the receptive fields (clusters) of the SOM. We used a SOM with a topology of 20×30 neurons (600 receptive fields) organized as a torus. The SOM was trained in 5×10^6 cycles. The parameter defining the decay of weight update during training was initialized with 1. The initial width of the Gaussian neighborhood function was 5. Distances were calculated as the Euclidean distance. From

the trained SOM we selected the 912 compounds assigned to the neuron containing the reference compound for the virtual screening process.

PhAST: The pharmacophore alignment search tool (PhAST) is a string-based approach to virtual screening.[27] It reduces each molecule to an unambiguous linear representation describing its pharmacophoric features—called 'PhAST-sequence'—in three steps: 1) each non-hydrogen atom in the structure graph is replaced by a potential pharmacophoric point symbol; hydrogen atoms are removed; 2) vertices of this pharmacophoric feature graph are canonically labeled, and 3) vertex symbols are concatenated into a string in increasing order of their canonical labels. For virtual screening, both the screening compound collection ('library') and the query molecules were converted and the resulting PhAST sequences were compared using pairwise global sequence alignment.[37] As a result, molecular similarity values are computed from the pairwise alignments, which were used for the retrieval of molecules with similar pharmacophoric features from a compound database. PhAST distinguishes between nine different potential pharmacophore points: positive charge; negative charge; aromatic; lipophilic; hydrogen-bond donor; hydrogen-bond donor and acceptor; hydrogen-bond acceptor and positive charge; hydrogen-bond donor and acceptor and positive charge; no interaction. The original version of PhAST uses the algorithm of Weininger et al.[38] for canonization. In this work we employed the algorithm by Prabhakar and Balasubramanian[39] (referred to as 'PhAST Prabhakar') and the Isomap algorithm[40] (referred to as 'PhAST Isomap'). PhAST Prabhakar was used with gap open penalty=5 and gap extension penalty=1; PhAST Isomap with gap open penalty=8 and gap extension penalty=1. With all versions of PhAST the published standard score matrix was used.[27] In contrast to the original version of PhAST, we calculated the alignment score normalized to the alignment length as a similarity measure between aligned sequences instead of sequence identity. These modifications were shown to be superior to the original approach.[41]

PRPS: Pseudoreceptor point similarity (PRPS) is a virtual screening tool bridging receptor- and ligand-based screening techniques.[28] Starting from a 3D conformation of a ligand, PRPS projects potential interaction points into the surrounding space mimicking a surrounding "idealized" receptor pocket. Location of interaction points depends on known preferred distances and angles of the respective hypothetical interaction, assumed to be possible at this position of the ligand. The type of an interaction point (hydrogen-bond donor, hydrogen-bond acceptor, π stacking ("aromatic")) is complementary to the respective potential pharmacophoric point of the ligand. The spatial arrangement of generated interaction points is then transformed into an alignment-invariant representation as a cross-correlation descriptor. PRPS compares two molecules by calculating the Euclidian distance between their descriptor representations. A PRPS model can be computed for a single ligand or for a set of multiple ligands. In the latter case the model is built based on an alignment of all compounds, and projected interaction points are weighted by the number of molecules that projected them to the same location.

ShaEP: ShaEP is a tool for 3D ligand-based virtual screening that evaluates the similarity between two molecules by means of spatial overlap in volume and calculated electrostatic potential fields.[29] Rigid body alignment of the molecules is performed to optimize overlaps. Ligand flexibility can be addressed implicitly by not only comparing a single conformation of both molecules but instead by performing an exhaustive pairwise comparison of conformation ensembles. For ShaEP screenings, up to 10 conformations of both the reference ligand and each screening compound were generated using the stochastic conformer generation routine of MOE. Partial charges for every conformation were calculated according to the MMFF94 parameter set available in MOE. Only the highest score of all pairwise comparisons was considered for the final ranking of screening compounds.

Homology model: A comparative protein model ("homology model") of SaTK was built using the web service of Swiss Model[42,43] in automated mode. The crystal structure of *Bacillus anthracis* thymidine kinase (PDB identifier: 2j9r, chain A) served as template. The query sequence was derived from *S. aureus* ATCC 700699 thymidine kinase (access number: NP_372643).

Automated ligand docking: Docking experiments were performed using the software GOLD[44] with the ASP scoring function. Residues F92, L116, D119, F120, F125, T155, R157, I170, I171, L172, V173, G174, and Y179 defined the binding site. Initial 3D conformations of docked compounds were calculated by CORINA prior to docking.

Microdilution assay: Minimal inhibitory concentrations (MICs) of the potential different thymidine kinase inhibitors alone and in combination with SXT against *S. aureus* strain ATCC 700699 and *S. aureus* ATCC 29213 in the presence of thymidine were determined according to Clinical and Laboratory Standards Institute (CLSI) guidelines with some modifications.[34] Therefore, a bacterial suspension (95 μL, exponential growth phase) of *S. aureus* strains (ca. 5×10^5 cells mL^{-1}) in cation-adjusted Mueller–Hinton broth (Becton, Dickinson and Company, Sparks, USA) supplemented with thymidine (200 μg L^{-1}; Sigma–Aldrich, Munich, Germany) and with or without trimethoprim/sulfamethoxazole (40 mg) in a ratio of 1:19 (both Sigma–Aldrich) was added to each well of a 96-well microtiter plate (Greiner, Monroe, USA). A solution (5 μL) of different potential thymidine kinase inhibitors in various dilutions was added to each well (range of final concentrations: 0.03125 to 128 mg L^{-1}). After 20 h of incubation at 37 °C, MICs were determined. Experiments were performed in triplicate.

[1] F. D. Lowy, *N. Engl. J. Med.* **1998**, *339*, 520–532.
[2] T. Kitahara, Y. Aoyama, Y. Hirakata, S. Kamihira, S. Kohno, N. Ichikawa, M. Nakashima, H. Sasaki and S. Higuchi, *Int. J. Antimicrob. Agents* **2006**, *27*, 51–57.
[3] G. Y. Zuo, G. C. Wang, Y. B. Zhao, G. L. Xu, X. Y. Hao, J. Han, Q. Zhao, *J. Ethnopharmacol.* **2008**, *120*, 287–290.
[4] F. W. Goldstein, *Clin. Microbiol. Infect.* **2007**, *13*, 2–6.
[5] S. Tsiodras, H. S. Gold, G. Sakoulas, G. M. Eliopoulos, C. Wennersten, L. Venkataraman, R. C. Moellering, M. J. Ferraro, *Lancet* **2001**, *358*, 207–208.
[6] M. Adra, K. R. Lawrence, *Ann. Pharmacother.* **2004**, *38*, 338–341.
[7] S. A. Grim, R. P. Rapp, C. A. Martin, M. E. Evans, *Pharmacotherapy* **2005**, *25*, 253–264.
[8] S. Besier, J. Zander, E. Siegel, S. H. Saum, K. P. Hunfeld, A. Ehrhart, V. Brade, T. A. Wichelhaus, *J. Clin. Microbiol.* **2008**, *46*, 3829–3832.
[9] R. A. Proctor, *Clin. Infect. Dis.* **2008**, *46*, 584–593.
[10] J. Zander, S. Besier, H. Ackermann, T. A. Wichelhaus, *Antimicrob. Agents Chemother.* **2010**, *54*, 1226–1231.
[11] J. S. Lockwood, H. M. Lynch, *JAMA J. Am. Med. Assoc.* **1940**, *114*, 935–939.
[12] C. M. MacLeod, *J. Exp. Med.* **1940**, *72*, 217–232.
[13] U. Kosinska, C. Carnrot, S. Eriksson, L. Wang, H. Eklund, *FEBS J.* **2005**, *272*, 6365–6372.
[14] P. Voytek, P. K. Chang, W. H. Prusoff, *J. Biol. Chem.* **1972**, *247*, 367–372.
[15] C. Carnrot, S. R. Vogel, Y. Byun, L. Wang, W. Tjarks, S. Eriksson, A. J. Phipps, *Biol. Chem.* **2006**, *387*, 1575–1581.
[16] E. Galanis, R. Goldberg, J. Reid, P. Atherton, J. Sloan, H. Pitot, J. Rubin, A. A. Adjei, P. Burch, S. L. Safgren, T. E. Witzig, M. M. Ames, C. Erlichman, *Ann. Oncol.* **2001**, *12*, 701–707.
[17] E. De Clercq, *Methods Find. Exp. Clin. Pharmacol.* **1980**, *2*, 253–267.
[18] W. H. Prusoff, M. S. Chen, P. H. Fischer, T. S. Lin, G. T. Shiau, R. F. Schinazi, J. Walker, *Pharmacol. Ther.* **1979**, *7*, 1–34.
[19] C. Carnrot, R. Wehelie, S. Eriksson, G. Boelske, L. Wang, *Mol. Microbiol.* **2003**, *50*, 771–780.

[20] U. Kosinska, C. Carnrot, M. P. Sandrini, A. R. Clausen, L. Wang, J. Piskur, S. Eriksson, H. Eklund, *FEBS J.* **2007**, *274*, 727–737.

[21] L. Stryer in *Biochemie* (Ed.: L. Stryer), Spektrum der Wissenschaft, Heidelberg, **1990**, pp. 627–653.

[22] J. Zander, S. Besier, S. H. Saum, F. Dehghani, S. Loitsch, V. Brade, T. A. Wichelhaus, *Infect. Immun.* **2008**, *52*, 2183–2189.

[23] R. Lam, K. Johns, K. P. Battaille, V. Romanov, K. Lam, E. F. Pai, N. Y. Chargadze, unpublished results.

[24] D. Segura-Peña, J. Lichter, M. Trani, M. Konrad, A. Lavie, S. Lutz, *Structure* **2007**, *15*, 1555–1566.

[25] a) T. Kohonen, *Biol. Cybern.* **1982**, *43*, 59–69; b) J. Zupan, J. Gasteiger, *Neural Networks for Chemists. An Introduction*, Wiley-VCH, Weinheim, **1999**.

[26] a) P. Schneider, G. Schneider, *QSAR Comb. Sci.* **2003**, *22*, 713–718; b) P. Schneider, Y. Tanrikulu, G. Schneider, *Curr. Med. Chem.* **2009**, *16*, 258–266; c) S. Renner, M. Hechenberger, T. Noeske, A. Böcker, C. Jatzke, M. Schmuker, C. G. Parsons, T. Weil, G. Schneider, *Angew. Chem.* **2007**, *119*, 5432–5435; *Angew. Chem. Int. Ed.* **2007**, *46*, 5336–5339.

[27] V. Hähnke, B. Hofmann, T. Grgat, E. Proschak, D. Steinhilber, G. Schneider, *J. Comput. Chem.* **2009**, *30*, 761–771.

[28] a) Y. Tanrikulu, E. Proschak, T. Werner, T. Geppert, N. Todoroff, A. Klenner, T. Kottke, K. Sander, E. Schneider, R. Seifert, H. Stark, T. Clark, G. Schneider, *ChemMedChem* **2009**, *4*, 820–827; b) Y. Tanrikulu, G. Schneider, *Nat. Rev. Drug Discov.* **2008**, *7*, 667–677.

[29] M. J. Vainio, J. S. Puranen, M. S. Johnson, *J. Chem. Inf. Model* **2009**, *49*, 492–502.

[30] A. Hopkins, C. Groom, A. Alex, *Drug Discovery Today* **2004**, *9*, 430–431.

[31] a) G. Schneider, M. Hartenfeller, M. Reutlinger, Y. Tanrikulu, E. Proschak, P. Schneider, *Trends Biotechnol.* **2009**, *27*, 18–26; b) G. Schneider, S.-S. So, *Adaptive Systems in Drug Design*, Landes Bioscience, Georgetown, **2002**; c) T. I. Oprea, *Curr. Opin. Chem. Biol.* **2001**, *5*, 384–389.

[32] a) T. I. Oprea, H. Matter, *Curr. Opin. Chem. Biol.* **2004**, *8*, 349–358; b) H. Eckert, J. Barorath, *Drug Discovery Today* **2007**, *12*, 225–233; c) G. Schneider, *Nat. Rev. Drug Discovery* **2010**, *9*, 273–276.

[33] K. Hiramatsu, H. Hanaki, T. Ino, K. Yabuta, T. Oguri, F. C. Tenover, *J. Antimicrob. Chemother.* **1997**, *40*, 135–136.

[34] M. Kuroda, T. Ohta, I. Uchiyama, T. Baba, H. Yuzawa, I. Kobayashi, L. Cui, A. Oguchi, K. Aoki, Y. Nagai, J. Lian, T. Ito, M. Kanamori, H. Matsumaru, A. Maruyama, H. Murakami, A. Hosoyama, Y. Mizutani-Ui, N. K. Takahashi, T. Sawano, R. Inoue, C. Kaito, K. Sekimizu, H. Hirakawa, S. Kuhara, S. Goto, J. Yabuzaki, M. Kanehisa, A. Yamashita, K. Oshima, K. Furuya, C. Yoshino, T. Shiba, M. Hattori, N. Ogasawara, H. Hayashi, K. Hiramatsu, *Lancet* **2001**, *357*, 1225–1240.

[35] CLSI. Methods for Dilution Antimicrobial Susceptibility Tests for Bacteria That Grow Aerobically; Approved Standard, 8th ed., M7A8, Clinical and Laboratory Standards Institute, Wayne, PA, **2008**.

[36] K. Pearson, *Philos. Mag.* **1901**, *2*, 559–572.

[37] S. B. Needleman, C. D. Wunsch, *J. Mol. Biol.* **1970**, *48*, 443–453.

[38] D. Weininger, A. Weininger, J. L. Weininger, *J. Chem. Inf. Comput. Sci.* **1989**, *29*, 97–101.

[39] Y. S. Prabhakar, K. Balasubramanian, *J. Chem. Inf. Model* **2006**, *46*, 52–56.

[40] J. B. Tenenbaum, V. de Silva, J. C. Langford, *Science* **2000**, *290*, 2319–2323.

[41] V. Hähnke, M. Rupp, M. Krier, F. Rippmann, G. Schneider, *J. Comput. Chem.* **2010**, DOI: 10.1002/joc.21574.

[42] K. Arnold, L. Bordoli, J. Kopp, T. Schwede, *Bioinformatics* **2005**, *22*, 195–201.

[43] Swiss Model: http://swissmodel.expasy.org/ (accessed 25.02.2010).

[44] G. Jones, P. Willett, R. C. Glen, A. R. Leach, R. Taylor, *J. Mol. Biol.* **1997**, *267*, 727–748.